JOURNAL OF SPACECRAFT AND ROCKETS
Vol. 42, No. 4, July–August 2005

Airframe–Propulsion Integration Methodology for Waverider-Derived Hypersonic Cruise Aircraft Design Concepts

Kashif H. Javaid* and Varnavas C. Serghides†
Imperial College London, London, England SW7 2AZ, United Kingdom

A design methodology employed for a practical preliminary-level integration of a conically derived hypersonic waverider airframe with its propulsion system is described. A Mach 9 baseline vehicle is generated using an inverse design approach and the streamline tracing method. Turboramjets are used to accelerate the vehicle from takeoff to a transition speed of Mach 5, where a scramjet takes over and accelerates the vehicle to a hypersonic cruise speed of Mach 9 at an altitude of 30 km as described by the design mission profile. The integration of the propulsion units and their inlets, with the airframe, are explored and demonstrated by approximately matching the thrust from the low-speed units to that from the high-speed ones. The propulsion–airframe integration forms part of the work toward developing a full practical design methodology for hypersonic cruise aircraft concepts.

Nomenclature

A	=	capture area
A/A^*	=	isentropic area ratio
ae	=	semiminor axis of inlet curve
be	=	semimajor axis of inlet curve
D	=	drag
F/m_0	=	specific thrust
H	=	height
h	=	altitude
I_{sp}	=	specific impulse
j	=	spanwise iterator
L	=	lift
L_{fore}	=	length of forebody
M	=	mach number
$\dot{m}$	=	mass flow rate
P	=	pressure
R	=	radius
Re_θ	=	Reynolds number based on inlet momentum thickness
S_t	=	length of shock train
T	=	temperature
V	=	velocity
W	=	width
w	=	local axial velocity
x	=	waverider radial distance from cone
z	=	waverider axial coordinate
α	=	turboramjet (TRJ) bypass ratio
γ_b	=	specific heat ratio
ϵ	=	bow shock angle
η_R	=	inlet total pressure recovery
θ	=	semispan angle, boundary-layer momentum thickness
π_F	=	TRJ total pressure ratio
ρ	=	local density
ψ	=	stream function
0	=	freestream
1	=	inlet capture
2–10	=	engine station numbers

Subscripts

c	=	cone surface
comb	=	combustor
eng	=	engine at inlet plane
i	=	inlet station
p	=	TRJ primary flow
r	=	radial
req	=	required engine airflow
s	=	shock position at given station/shock train
t	=	total
wing	=	wing curve
x	=	axial distance

Introduction

A TECHNICALLY viable solution for the design of vehicles capable of hypersonic flight demands an accurate integration of the propulsion system with the lower part of the vehicle airframe. The freestream capture area must be large for the engine to generate sufficient thrust at high altitudes and the nozzle exit area should be large for sufficient expansion. As was seen by the recent successful test by NASA's X-43A experimental research vehicle,[1] the forebody of that aircraft served as the compression surface for the efficient operation at hypersonic speeds and the afterbody functioned as an extension to the nozzle expansion surface. The entire undersurface for hypersonic vehicles is used for the propulsion system due to the high level of interaction between the designs of these vehicle components.

Hypersonic vehicles will serve a valuable role for both commercial and military applications in future aerospace operations. Without existing baseline vehicles or practical design experience in this field, the development of operational hypersonic vehicles has challenged the aerospace community for many years. The study of hypersonic flow around a vehicle differs from that of supersonic/subsonic flow due to the high stagnation temperatures and enthalpies experienced. The vehicle will travel along a high-dynamic-pressure trajectory, with high heat transfer implications and a change in the near-field characteristics of air. This can directly affect combustion of a supersonic stream. Advances in topics such as aerothermodynamics, combined cycle propulsion systems, high-temperature materials, cost, and so on have, however, expedited the design challenge.[2] The potential applications for such a vehicle span from a reusable launch vehicle for cost-effective access to space to high-speed air transportation and rapid global response. The latter is the focus of the present study and represents a hypersonic endoatmospheric cruise vehicle capable of delivering a payload to any point on the globe.

Presented as Paper 2004-1201 at the AIAA 42nd Aerospace Sciences Meeting, Reno, NV, 5–8 January 2004; received 4 March 2004; revision received 8 June 2004; accepted for publication 9 June 2004. Copyright © 2004 by the American Institute of Aeronautics and Astronautics, Inc. All rights reserved. Copies of this paper may be made for personal or internal use, on condition that the copier pay the $10.00 per-copy fee to the Copyright Clearance Center, Inc., 222 Rosewood Drive, Danvers, MA 01923; include the code 0022-4650/05 $10.00 in correspondence with the CCC.

*Research Student, Department of Aeronautics, South Kensington Campus. Student Member AIAA.

†Lecturer, Department of Aeronautics, South Kensington Campus. Senior Member AIAA.

A good measure of the aerodynamic efficiency of an aerospace vehicle is its L/D ratio and specific impulse. The vehicle cruises at high altitudes where the atmosphere is thin and requires a large mass capture area for rapid combustion and thrust generation. The L/D ratio becomes particularly important in selecting a suitable airframe to achieve a global range. High aerodynamic and propulsion efficiency are required at cruise Mach numbers, leading to slender aerodynamic shapes with the potential of integrating the highly specialized propulsion system.

One class of vehicles that has demonstrated high values of L/D at high speeds compared to conventional lifting-body designs are waveriders, which also offer a good degree of volumetric efficiency.[3] A waverider is defined as a vehicle that generates lift from its bow shock wave that is attached all along the leading edge. The compression surface is isolated from the top surface such that they can be designed independently. The high pressure behind the shock does not leak around the leading edge to the top surface if the shock wave is attached and preserved. The waverider is inversely designed from a known generating flowfield. The method employed in this study is computationally quick to generate and is therefore well suited for optimization studies allowing rapid exploration of multiple designs.

For takeoff and landing capability, various propulsion concepts have been proposed to address the Mach regime from brakes release to Mach 5 or 6. The rocket-based combined-cycle (RBCC) engine combines the characteristics of both airbreathing and rocket engines. It produces high specific impulse compared to a rocket engine and high thrust-to-weight ratio compared to an airbreathing engine.[4] The integration of an RBCC engine with an osculating cone waverider was discussed in Ref. 5 and was shown to produce rapid results for the aerodynamic performance.

For this study, a turbine-based combined-cycle (TBCC)-type powerplant was adopted as a possible candidate to accelerate a vehicle from brake release until transition to a high-speed powerplant that can accelerate the vehicle to the desired hypersonic cruise Mach number. Here, the low-speed powerplant is a TRJ and the high-speed powerplant is a scramjet (SJ). In this paper, the term low-speed will be used to describe flight speeds less than Mach 5, whereas high-speed will imply speeds above Mach 5. The TRJ is rendered inoperable at large Mach numbers due to high-temperature effects and inefficient compression, which necessitates the use of an SJ. For TRJ systems, questions concerning the arrangement of the propulsion system with the high-speed part is resolved with consideration of fuel issues, aerodynamic design of inlets, and nozzles, together with thermal analysis of these components, which is a major consideration.

The main objective of the current research program is to develop an initial design methodology for airbreathing cruise vehicles that will be capable of sustained hypersonic flight, with horizontal takeoff and landing capability and global reach potential. Using airbreathing engines, the need for carrying an onboard oxidizer is also avoided, resulting in weight savings, reduced complexity, and low ground support. Reusability will therefore be enhanced, leading to fast turnarounds and quick response times.

Airframe–propulsion integration is a complex process requiring analysis of multiple systems concurrently to obtain optimum overall performance. The external surfaces affect both lifting capability and volumetric capacity, while the nozzle determines the thrust vector. The success of such a vehicle is therefore critically dependent on the tight integration of these propulsion units and their inlets with the waverider airframe. Notable challenges are associated with efficient operation of multiple engines with regard to flowpath integration and performance requirements.

As part of the overall design methodology development, this paper seeks to assess the potential of installing multiple engine flowpaths onto a waverider airframe with analysis of the performance requirements. In particular, emphasis has been placed on low-speed design characteristics and the development of a fast and user-friendly code. In this paper, results are presented for the smooth thrust transition between low-speed and high-speed engines by using simple physics models for propulsion and geometry to maximize aerodynamic performance with a discussion on the arrangement of inlets for the two

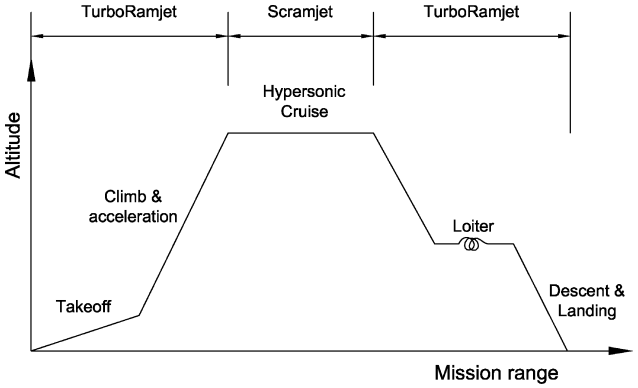

Fig. 1 Design mission profile for hypersonic cruise aircraft.

powerplants. A description of the design methodology is given in the following section. For cruise-type vehicles, considered in this study, the objective function is to maximize the range for a given payload so that it must yield a high value of the product of I_{sp} and L/D.

A target design study for the airframe–propulsion integration relevant to the present analysis is illustrated in the mission profile of Fig. 1. The vehicle will be designed for a horizontal takeoff followed by an accelerated climb using an array of TRJs until the desired cruise altitude specified by the user is achieved at Mach 5. Before this, the TRJ propulsion system will continue operating in parallel with the SJ, and when thrust matching is achieved (near Mach 5), the airflow to the TRJ will be shut off. The SJ will then throttle up and the aircraft will begin a constant-altitude acceleration to the desired cruise Mach number. At the end of the cruise segment, the vehicle will slow down and revert to TRJ power, descend to a specified loiter altitude, deliver its payload, and then fly to a base for refueling.

Development of Methodology

The maturity of a hypersonic waverider is contingent upon advances in computational techniques that can account for the complex three-dimensional viscous flowfields and complex wave systems around the vehicle without the expensive computational cost attributed to computational fluid dynamics (CFD) methods. For rapid results, analytical methods are required that produce an acceptable level of accuracy. Analytical techniques are a necessary alternative to define the design space and establish feasibility criteria to constrain the operating domain. This is especially important given that hypersonic vehicle design is dependent on the amalgamation of several aircraft components and tradeoffs among them. For example, tradeoffs in forebody and nozzle length determine the position of the engine along the vehicle. A shorter nozzle length results in reduced thrust due to an underexpanded nozzle flowfield. There is also an inherent tradeoff between producing thrust and lift due to the strong coupling between the engine and airframe.[6] As the vehicle flies along a trajectory, tradeoffs among dynamic pressure for propulsion, heating, and pressure loads need to be analyzed.

As mentioned earlier, the relationship between a vehicle's airframe and propulsion system is closely linked such that modeling their interaction will define the success of a proposed concept. These modeling methods are developed from experimental data and fundamental principles. The advantages of rapid performance estimation were the drive behind early methodologies that addressed the full Mach range.[7] These, however, considered either simple geometric shapes not accounting for the complex flowfield or focused on singular design cases.[8] Improved studies have shown that airbreathing engines can be efficiently integrated with various waverider airframes. Included in these was a supersonic combustion ramjet (SJ) integration with a conically derived waverider[9] for on-design hypersonic Mach numbers. Also included was an SJ integration on an osculating-cone-based waverider,[10] which addressed both on- and off-design issues and showed that a greater usable volume is produced for this type of vehicle with comparable L/D ratios.

To this end, a methodology is being developed as part of a Ph.D. program at Imperial College London. Hypersonic Interactive Combat Aircraft Design (HICAD) is an interactive computer software with the aim of rapidly generating hypersonic configurations from a small set of initial parameters. HICAD is a visual environment written in C++ and MFC[11] and consolidates various preliminary design tools and mathematical models to facilitate the design of practical operational aircraft. This allows for fast analysis and the study of a wide range of hypersonic vehicle concepts, significantly reducing the initial design cycle time compared to detailed component CFD analyses, which are too slow and expensive for the preliminary design level. Key elements of the present study are 1) design of a baseline waverider vehicle, 2) analysis and integration of propulsion systems, and 3) performance of key design trades such as mission scenario, systems packaging, and takeoff and landing requirements.

The design begins by performing an initial sizing process that is dependent on user-selected basic requirements such as cruise Mach number and altitude. A definition of the mission profile determines the aircraft constraints, range, and therefore fuel required, number of engines, and so on. This study focuses on an uninhabited vehicle, which is a likely development strategy considering the inherent complexities associated with accommodating a human pilot on board, although future versions of HICAD will be capable of dealing with piloted missions. The airframe–propulsion integration has been discussed in this paper to highlight the potential applicability of such a methodology.

The waverider design is addressed first with a calculation of L_{fore} using a streamline tracing method. The cruise Mach number, altitude, and geometric inputs such as the generating curve in the inlet plane are required for this computation. Given an acceptable L_{fore}, the SJ inlet size is determined for the on-design case from a predefined combustor pressure ratio. An iteration is performed that outputs optimum values for inlet ramp angle, inlet height, and flow properties at the inlet–combustor junction and the capture area. The SJ computation then proceeds with an ideal combustor analysis to estimate the flow entry properties to the nozzle. The two-dimensional method of characteristics is used to calculate the expansion flowfield from the combustor exit to the exit plane at the trailing edge of the vehicle. This fixes the total waverider length. The performance of the propulsion system can be determined in terms of thrust and specific impulse.

The wing section that extends to the trailing edge of the vehicle is then calculated subject to geometric constraints imposed[12] on the design space to maximize L/D. This completes the on-design case. Following that, the low-speed propulsion analysis is performed by selecting a TRJ design condition and using the model reported by Heiser and Pratt.[13] Performance parameters are determined for $0 \le M_0 \le 5$. The inlet is then designed for the TRJ by using an off-design cycle analysis code, OFFX,[14] that computes the required mass flow. Iteration is required to find an inlet size that will deliver the desired thrust during the TRJ/SJ transition stage. This is discussed in further detail in a later section.

The HICAD concept is illustrated in the flowchart of Fig. 2, which shows the highly integrated nature of the design process and provides further information on the computational steps required for a complete design.

One of the most important aspects of a vehicle design of this nature is to incorporate optimization into the analysis. This can account for the nonlinear interaction between aircraft complements. Such multidisciplinary optimization has been shown[15] to produce significant performance benefits over nonoptimum concepts. For the purpose of this paper, optimization has been performed on the external vehicle geometry in establishing a maximum L/D shape for given geometric constraints, although HICAD will ultimately be extended to analyze the synergy among aerodynamics, propulsion, control, and packaging and to reduce the uncertainty with economics, trajectory, and nonlinear relationships. The preliminary level of design will be linked with a parametric computer-aided design (CAD) system[16] for two-way information sharing that is, a change in user requirements will send data to the CAD system and vice versa.

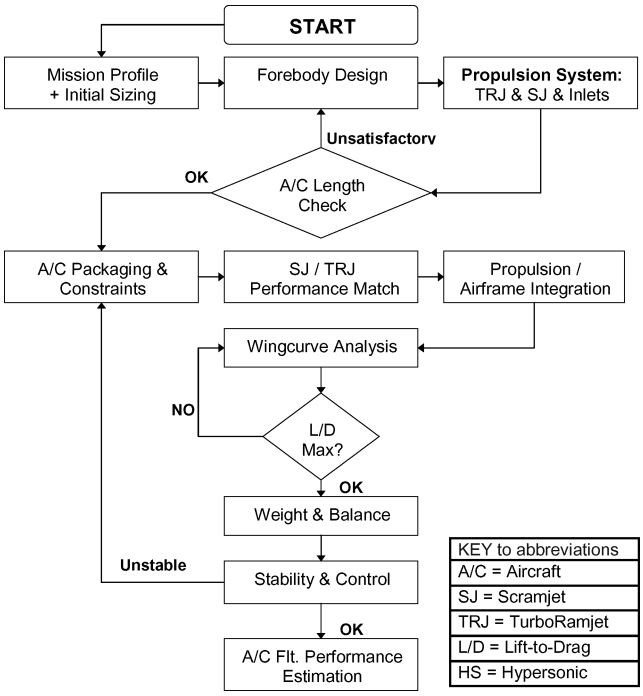

Fig. 2 HICAD flowchart illustrating the complete design process for hypersonic vehicle design.

The vehicle component models are discussed in the remainder of this paper and are used to calculate aerodynamic performance and lift. The models are adequate for the conceptual level of design, ensuring fast computational time for practical optimization.

Waverider

Highly integrated airframes provide both maximum inlet capture area and nozzle expansion. The forebody design directly affects the inlet performance and is maximized if the inlet is located within the forebody flowfield. This increases the pressure ratio and maximizes the inlet capture area for efficient inlet performance. The overall dimensions of the inlet are reduced, thereby reducing the drag, and provide greater flow uniformity at the combustor face. The design affects vehicle aerodynamics and propulsive performance. The forebody must provide the desired mass flow to the inlet as well as minimize inlet flow distortion.

Using a right-circular cone, the flowfield of this simple shape is calculated and used as the generating flowfield for the inverse design process of the waverider. The conical flowfield is determined by solving the Taylor–Maccoll equation using a fourth-order numerical Runge–Kutta technique[17]:

$$\frac{\gamma-1}{2}\left[1-V_r'^2-\left(\frac{\mathrm{d}V_r'}{\mathrm{d}\theta}\right)^2\right]\left[2V_r'+\frac{\mathrm{d}V_r'}{\mathrm{d}\theta}\cot\theta+\frac{\mathrm{d}^2V_r'}{\mathrm{d}\theta^2}\right]-\frac{\mathrm{d}V_r'}{\mathrm{d}\theta}\left[V_r'\frac{\mathrm{d}V_r'}{\mathrm{d}\theta}+\frac{\mathrm{d}V_r'}{\mathrm{d}\theta}\frac{\mathrm{d}^2V_r'}{\mathrm{d}\theta^2}\right]=0 \tag{1}$$

where V_r and θ are the two independent variables and $V_\theta = \mathrm{d}Vr'/\mathrm{d}\theta$. The cone is an axisymmetric shape, and so determining the flowfield in one plane is sufficient for other spanwise stations, which reduces the computational cost. An elliptical inlet curve is specified in the inlet plane[12] for a number of points in the spanwise direction; ψ is determined at each of these points using the following equation:

$$\psi(j) = 2\pi \int_{x_{\text{cone}}(j)}^{x_i(j)} \rho(z_i, x)\cdot w(z_i, x)\cdot x\,\mathrm{d}x \tag{2}$$

The streamlines are traced forward until the generating shock is intersected and this method is repeated for each point along the inlet curve up to the half-span of the engine, which is specified as

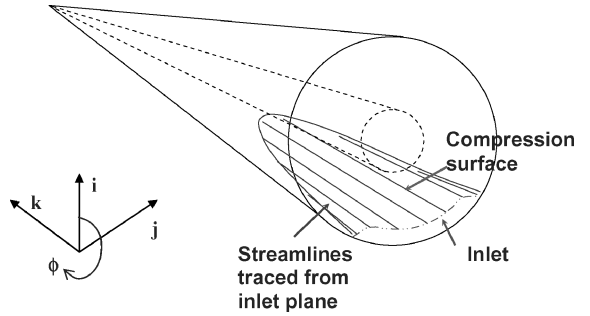

Fig. 3 Forebody generation using an inverse design approach starting at the inlet plane; adapted from Ref. 9.

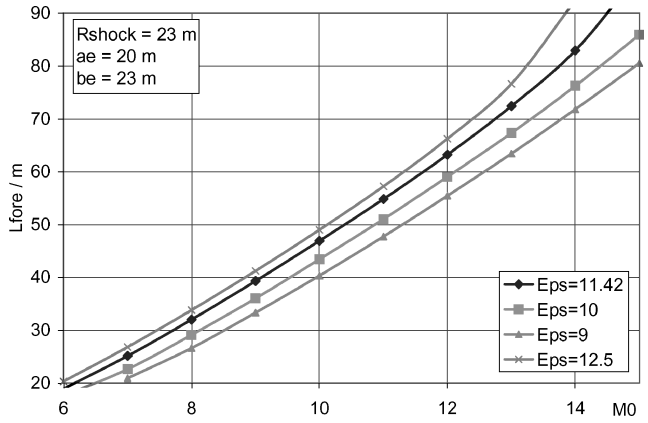

Fig. 4 Forebody length variation with different bow shock angles.

a user input in HICAD. The resulting shape is the lower surface of the waverider forebody for the engine span section. For the present analysis, the top surface is simply freestream streamlines traced back toward the tail of the waverider (Fig. 3).

The method of tracing streamlines forward until shock intersection ensures that the leading edge of the waverider is attached to the shock. This reduces pressure leakage and maximizes the mass flow capture for combustion.

L_{fore} is dependent on the shape of this inlet curve, which is defined by ae, be, and the R_s, at the inlet plane as illustrated in Ref. 12. L_{fore} variation with Mach number is shown in Fig. 4 for varying ϵ. In general, the length appears to increase linearly with M_0 for given values of ae, be, and R_s.

The wing cross section of the waverider is defined by a set of points in the inlet plane and a third-order polynomial fit through these points, which establishes a wing curve. The ψ values at each of these points are calculated using Eq. (2) and the streamline tracing method generates the remaining lower surface of the vehicle. Figures 5 and 6 illustrate the wing curve and the main engine span section of a Mach 9 waverider example.

High-Speed Propulsion

Research efforts[18–20] suggest that an SJ offers the greatest near-term development potential for hypersonic Mach numbers. Hydrogen was selected as the fuel for the SJ due to its higher performance yield and greater heat sink capacity. The fuel will be used for cooling the leading edges of the vehicle as needed. It also has high values of heat of combustion.

Scramjet Inlet

Analysis of the waverider flowfield indicates that the bow shock alone does not provide sufficient compression for desirable SJ combustor entrance properties. A two-dimensional single planar ramp has therefore been integrated with the lower surface of the waverider, forward of the cowl lip and with the same width as the engine in the inlet plane. The ramp shock produces, at least, the same pressure ratio as the bow shock. The ramp is positioned such that a

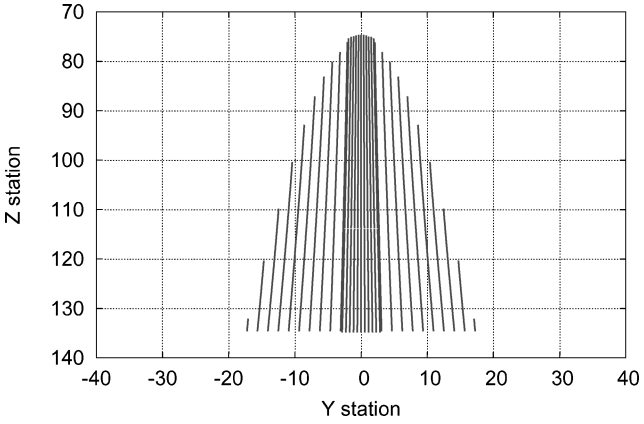

Fig. 5 Mach 9 example of waverider shape (plan view).

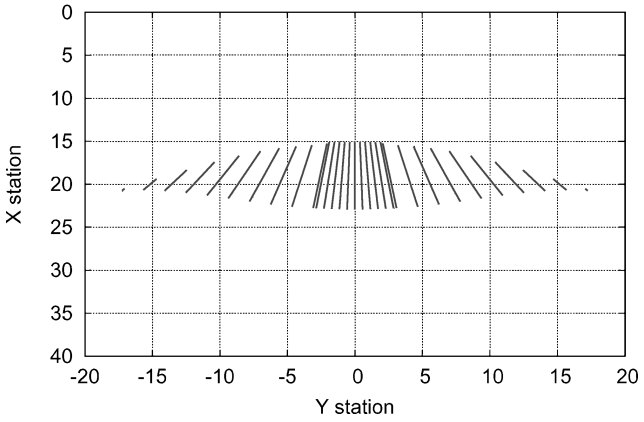

Fig. 6 Mach 9 example of waverider shape (front view).

second generating shock impinges on the cowl lip, as with the bow shock, which reflects, and this reflection cancels on the shoulder of the combustor upper wall. This shock-on-lip condition provides the maximum mass capture. The variable geometry inlet ramp system not only provides the desired pressure recovery as given by Billig[20] in Eq. (3),

$$P_i/P_0 = -8.4 + 3.5M_0 + 0.63M_0^2 \tag{3}$$

but transitions the inlet flowfield from three to two dimensions, providing greater flow uniformity for the combustor as the former creates boundary-layer growth and separation. The forebody flowfield is mass-averaged to enable a two-dimensional oblique shock calculation to be carried out for the ramp and combustor entrance conditions.

The entire length of the waverider undersurface can be considered part of the propulsion system. The forebody behaves as the precompression system and the afterbody acts as an extension to the nozzle. The ramp angle is varied iteratively until this compression ratio is achieved and always maintains the shock-on-lip condition for a given on-design M_0, which sets the height of the inlet in the inlet plane as shown in Fig. 7. The area of the inlet is determined by setting a value for W_{eng} at the inlet plane.

Combustor

The station numbers are indicated in Fig. 7 and represent the different stages in the design of a dual-mode SJ combustor. The flow at station 2 has been compressed by the bow and ramp shock and the reflected shock off the cowl lip. The conditions here form the start conditions for the combustor. Between stations 2 and 3, a constant-area section known as the isolator prevents undesirable inlet–combustor interactions, namely inlet unstart, by containing the precombustion shock structure. A significant problem in practical SJ operation is maintaining the pressure at station P_2 above the combustor backpressure P_3; otherwise, flow separation can occur

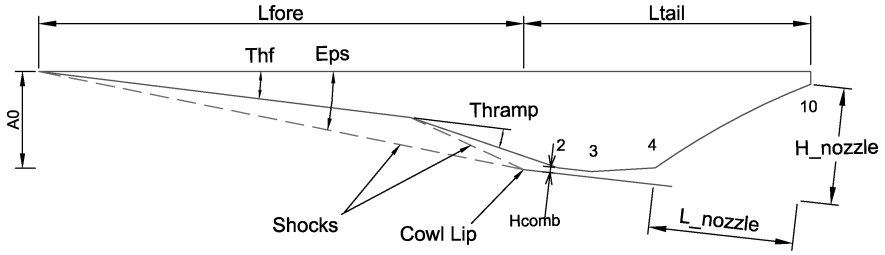

Fig. 7 Key geometric parameters in waverider design.

due to thermal occlusion. A simple quadratic relationship is used to find S_t for given inlet conditions based on experimental data:

$$\frac{S_t\left(M_2^2-1\right)Re_\theta^{\frac{1}{4}}}{D(\theta/D)^{\frac{1}{2}}}=50\left(\frac{P_s}{P_4-1}\right)+170\left(\frac{P_s}{P_4-1}\right)^2 \quad (4)$$

The existence of the shock train is dependent on the character of the boundary layer and whether or not separation occurs. The equation is applied to the design of the isolator and combustor.

The shock train exists between stations s and 2. At $M_0 > 8$, the heat release is not sufficient to choke the flow and the shock train disappears.

If the combustor length is too long, the takeoff weight increases and specific impulse decreases. The length cannot be shorter than that required for establishing complete mixing of fuel and air to produce the desired stoichiometric conditions. Because the flows within these combustors are supersonic, the mixing and residence time available for reaction are reduced compared to subsonic combustors. Its length is estimated using an analytical expression for the reaction time as a function of combustor entrance conditions.[5]

One of the keys for a successful design of an SJ combustor is the proper mixing of hydrogen fuel. The mixing length is a boundary condition for the separation and reattachment process. Oblique shocks present in the combustor can cause separation, and this can be predicted by using boundary-layer separation criteria, $M_d/M_u < 0.762$, to approximate turbulent boundary layers.[20] The length required for mixing can be estimated using empirical correlations given in Ref. 21.

In a dual-mode combustion system, both subsonic and supersonic combustion can occur within the same engine geometry. In ramjet mode, the transition from supersonic to subsonic flow is accomplished by means of an isolator. For burner entry flow to be subsonic, the flow must be choked. Downstream, this causes a large backpressure P_3 at burner entry and a normal shock train exists. A choked thermal throat can exist with the correct choice of A_x, fuel–air mixing, and combustion. During supersonic combustion, no physical throats are necessary but the isolator still serves a purpose by containing an oblique shock train resulting from heat addition in the combustor; this prevents inlet unstart. A control volume analysis of the isolator is carried out with reference to the work reported by Heiser and Pratt[13] and the minimum length is that given by the aforementioned shock train equation. The height of the isolator is represented by H_i.

Combustion occurs between stations 3 and 4 and fuel is injected at station 3. M_x is modeled using quasi-one-dimensional analysis based on calorically perfect gases with prescribed specific heat ratios. The SJ is modeled using quasi-one-dimensional equations based on Shapiro's formulation[22] for frictionless flow. Flame-holding and stabilization are neglected because their analysis would require CFD computations. The following ordinary differential equation for frictionless flow without mass addition but with a change A and T_t due to heat addition is solved step by step by using a fourth-order Runge–Kutta technique:

$$\frac{\mathrm{d}M_x}{\mathrm{d}x}=M_x\left\{\frac{1+[(\gamma_b-1)/2]M_x^2}{1-M_x^2}\right\}\left[-\left(\frac{1}{A_x}\frac{\mathrm{d}A_x}{\mathrm{d}x}\right)+\frac{1+\gamma_bM_x^2}{2}\left(\frac{1}{T_{tx}}\frac{\mathrm{d}T_{tx}}{\mathrm{d}x}\right)\right] \quad (5)$$

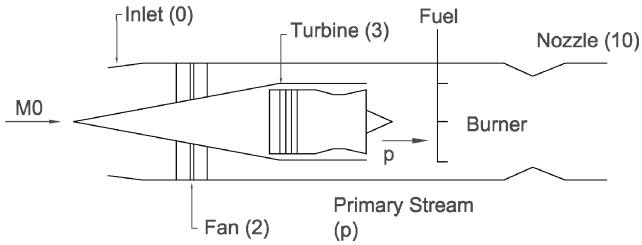

Fig. 8 Schematic of TRJ propulsion system.

Given that the combustor undergoes a user-defined change in A_x and an increase in T_{tx} due to heat addition, then Eq. (5) can be used to calculate the variation of thermodynamic properties. T_{tx} is determined by a rational function, and the thermophysical properties such as pressure, temperature, and velocity are obtained by using Shapiro's useful integral relations. This is based on calorically perfect gases with prescribed specific heat ratios, frictionless flow without mass addition, and constant-pressure heat addition.

Other assumptions made in the combustor analysis[23] include the following. The engine is a rectangular modular engine that attaches directly to the vehicle undersurface to simplify integration issues. The area change of the combustor, A_x, is a linear divergent section with an expansion ratio of 2:1 and heat addition occurs at constant pressure. The concept is likely to use swept compression surfaces and fuel-injector struts to provide low inlet starting speed and good internal performance throughout the SJ operating speed range. In-stream fuel injection is used to minimize combustor length and heat flux to the internal surfaces. Uniform two-dimensional flow exhausting from a single combustor exit was assumed to represent the engine package.

The one-dimensional model with effects of finite rate chemistry has previously been shown[21] to generate sufficiently accurate results for preliminary vehicle analysis with a relatively short computational time. The primary objective of such design codes remains the ease of computation.

Low-Speed Propulsion

A TBCC system was used to accelerate the vehicle from standstill to SJ transition. Existing research studies[24–27] examine the potential of a TRJ to meet this requirement. Idealized cycle analysis of a TRJ was carried out using the method described by Heiser and Pratt.[13] It assumes no friction and heat transfer to the walls and the flow is treated as steady and compressible. The TRJ generates static thrust at takeoff and subsonic speeds by mechanically compressing the air for stable combustion of fuel. The prominent components making up an axisymmetric TRJ are illustrated in the schematic of Fig. 8. This level of analysis is deemed suitable for the preliminary level of design especially during the development of the HICAD methodology.

The core of the engine contains a turbojet, which produces high-temperature and high-pressure gases. The turbojet flow is referred to as the primary stream because the turbine operates independently of the flight conditions. The turbines operate to provide power to the fan, which takes air from the inlet and produces a pressure ratio. The compression process to the fan inlet and turbine is treated as isentropic and there is no loss in efficiency between the two. Fuel

is mixed and the combustion process drives the turbine. The airflow around the core turbojet is mixed with the primary stream of the turbine, which increases the total temperature of the airflow.

The static pressure of the airflow and primary flow through the turbojet are equal. By equating the mixer with the main burner, fuel can be burned from the primary flow. This combustion of injected fuel is therefore analogous to afterburning in a turbojet. The influence of the fan on the airflow is defined by $\pi_F = p_{t3}/p_{t2}$. The method requires inputs for p_{tp}/p_0 and T_{tp}/T_0 as a function of the primary flow. The choices of these variables form part of an optimization procedure that results in suitable values until the desired I_{sp} and thrust are achieved for the $M_0 = 5$ SJ transition speed.

Next α is computed, which calculates the ratio of the airflow from the fan to the primary flow and is given by the following expression:

$$\alpha = T_{tp}/T_0 \cdot T_0/T_{t0}\left[1 - (\pi_F \cdot p_{t0}/p_0 \cdot p_0/p_{tp})^{(\gamma-1)/\gamma}\pi_F^{(\gamma-1)/\gamma} - 1\right] \tag{6}$$

When M_0 becomes large, α eventually reaches zero as shown in Fig. 9. This occurs when the quantity $\pi_F(p_{t0}/p_0) = p_{tp}/p_0$ in the numerator of Eq. (6). At this point the device is considered to behave like a rocket because the flow is entirely due to the primary flow and so airbreathing performance measures such as F/m_0 are no longer valid. For the purpose of this study, this is considered to be the limit of the TRJ model.

To achieve $M_0 = 5$, α needs to remain nonzero within the Mach range considered. If the military specification (MIL-E-5008B) for the total pressure recovery p_{t2}/p_{t0} is applied to the fan airflow for supersonic M_0, then this limit point can be delayed:

$$p_{t2}/p_{t0} = 1 - 0.075(M_0 - 1)^{1.35} \tag{7}$$

Furthermore, the diminishing P_0 that accompanies flying at increasing altitudes increases the value of p_{tp}/p_0 and T_{tp}/T_0, which has a favorable effect in achieving higher Mach numbers under TRJ power.

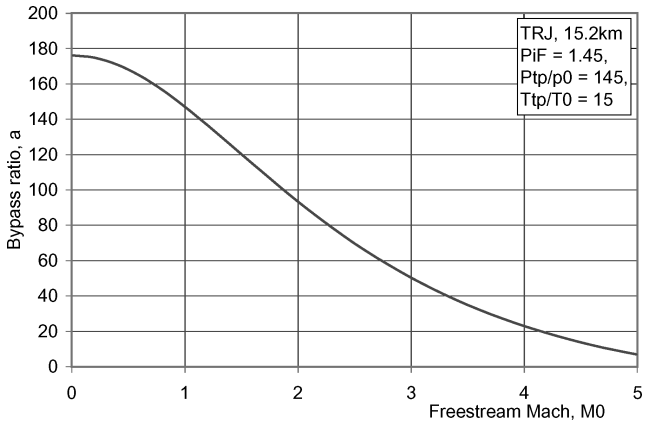

Fig. 9 The limit of the airbreathing segment indicated by the bypass ratio tending to zero.

For a smooth thrust transition between the TRJ and SJ engines, thrust matching needs to be achieved by varying the low-speed engine parameters within specified constraints, which include a peak value of $I_{sp} = 4000$ s from the available literature. This in turn provides data for F/m_0 as a function of h. The TRJ F/m_0 is found at the desired SJ transition point at $M_0 = 5$ and $h = 30$ km, and a value for $\dot{m}_0$ is determined to achieve the desired thrust in newtons for the SJ. This is also dependent on the number of engines, with a limit currently placed on four engine units. The design $\dot{m}_0$ cannot be too large; otherwise, the size of the inlet $A_{0_{ref}}$ becomes too large. I_{sp} is a function of the specific thrust given by the following equation:

$$I_{sp} = 1/g_0(f + 1/\alpha) \cdot F/\dot{m}_0 \tag{8}$$

where $g_0 = 9.81$ m/s^2.

For the low-speed segment of the mission, the TRJ analysis begins by determining the specific thrust at different altitudes using an idealized analysis. The size of the low-speed inlet is then calculated from the design M_0, h, and $\dot{m}_0$ variation with h using an external code that is integrated with HICAD. The required area ratio with respect to the design A_0 is plotted for different altitudes, and the most demanding $\dot{m}_0$ and h values are used to size the inlet. For the majority of cases studied that point was at Mach 5/cruise altitude transition to SJ mode. Once the inlet size and ramp angles are determined for the off-design conditions, fuel and other systems are accommodated into the vehicle's volume.

After achieving the desired performance matching of the low-speed and high-speed engine, a suitable external compression inlet needs to be designed for the TRJs. The inlet should 1) provide the necessary airflow for the TRJ from low-subsonic to high-supersonic flight conditions at all altitudes considered, 2) deliver high η_R, 3) ensure off-design conditions are fully met, and 4) minimize losses. In particular, the defined inlet should provide the necessary $\dot{m}_0$ to achieve the desired thrust for SJ transition. An off-design cycle analysis code, OFFX,[14] is used to determine the corrected engine airflow vs both M_0 and h. OFFX defines the requirement of the inlet in terms of its total pressure ratio based on Eq. (7) and $\dot{m}_0$.

Four successive variable geometry compression ramps represent the low-speed inlet system, one of which is the forebody ramp angle shown in Fig. 10. This was selected to generate good values of η_R over the desired flight-speed range while maintaining the shock-on-lip and sonic throat conditions. During off-design operation, the variable geometry ramps will maintain the shock on lip such that the shocks will not translate downstream of the inlet plane. This can cause boundary-layer separation and increased heating.

The inlet design begins with an analysis of the required inlet airflow.[14] As part of the multidisciplinary nature of the methodology, OFFX can be operated from within HICAD. By selecting a TRJ sizing point of $M_0 = 2.5$ at $h = 15.2$ km with $\dot{m}_0 = 136.1$ kg/s, the corresponding values of A_0 are calculated using OFFX at any other specified M_0 and h. Other variables used for optimization include the fan compressor ratio. The design case determines the reference area $A_{0_{ref}}$ and, using $\dot{m}_0$ vs M_0 data from OFFX at different h, an

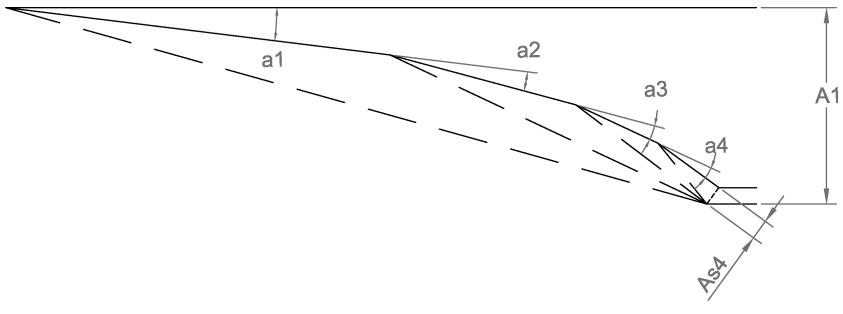

Fig. 10 TRJ inlet at Mach 5 and $h = 30$ km.

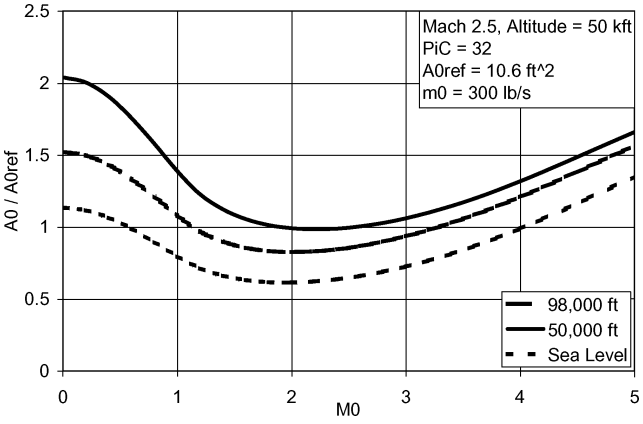

Fig. 11 Required inlet airflow at various altitudes.

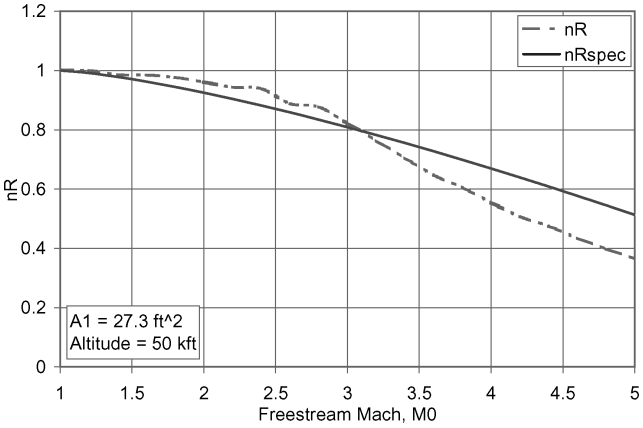

Fig. 12 Intake loss associated with a four-ramp inlet system.

airflow requirement plot $A_0/A_{0_{\text{ref}}}$ is produced like that shown in Fig. 11.

This figure presents information to select the flight condition at which the mass flow requirement at a particular Mach number is the greatest. The area ratio A_{0_i}/A_{s4} is then determined by the following equation given that $\eta_R = P_{t5}/P_{t0}$:

$$\frac{A_{0_i}}{A_{s4}} = \eta_R \frac{A/A^*|_{M_0}}{A/A^*|_{M_5}} \tag{9}$$

The required throat area A_{s4} can then be determined from $A_{s4} = A_{0_{\text{ireq}}}/A_{0_i}/A_{s4}$. Finally A_1 is calculated from geometry for a given value of A_{s4}. The value of A_1 is a function of the geometric ramp angle configuration and its final value is found when the highest value of η_R is achieved and M_4 is greater than unity, thus providing subsonic flow for the combustor.

Having determined $A1$, the ramp angles for the range of Mach numbers that lead to the best pressure recovery can be found. Given the large number of possible ramp angles, the selected configuration is based on equal strength shocks translating as an equivalent total pressure ratio across each shock. The pressure recovery at the design point should, at least, exceed Eq. (7) (Fig. 12).

The pressure recovery graph shown in Fig. 12 has a total flow turning angle of 36 deg at Mach 5 and 30 km. The pressure recovery can be improved by allowing a greater turning angle in this case but this will increase drag.

Nozzle

The design of the nozzle is primarily governed by stability and thrust requirements. The length and height of the nozzle, as shown in Fig. 7, are determined by subtracting the dimensions of the forebody and combustor length from the total vehicle length, which is set at 60 m for the purpose of this study. The combustor exit flow is treated as steady and irrotational and is considered to be uniform across the span of the engine, maintained by holding a constant spanwise upper wall angle. The contour of the nozzle is defined by a third-order polynomial curve and by setting the initial and final wall angles. The characteristic equations are considered hyperbolic and the two-dimensional method of characteristics can be used to compute the nozzle flowfield.[17] The value of the upper wall angle is solved iteratively so that the length and height of the nozzle are constrained by the available dimensions. This nozzle analysis and lift generation are discussed in Ref. 28. The expansion surface then contributes to thrust, lift, and pitching moment of the vehicle.

Numerical Optimization

The interaction of a multivariable system will result in large nonlinear uncertainties; to produce efficient integrated concepts, optimization of the system becomes essential.

The method adopted for obtaining a set of parameters producing a vehicle configuration subject to geometric constraints on the wing curve was the nonlinear simplex method of Nelder and Mead[29] given that it has been used successfully in the past in various airframe–engine integration studies.[15] The method minimizes an objective function though the use of simplexes and is very useful because the evaluation of function derivatives are not required. In this case, the objective function was a subroutine containing the methods to calculate the wing curve and the performance of the SJ. To minimize a function maximization, the subroutine's output is forced negative. If the result exceeds any of the constraints, a large value is passed, which alters the working domain of the simplex. A series of seven points was encapsulated by the simplex method and the points represent the defining geometric parameters in the inlet plane. These constraints are outlined in Ref. 12. In addition, the optimizer returned a nonfeasible vehicle if the points either intersected the cone or fell beyond the shock surface. For the purpose of this study, all vehicles were constrained to 60 m.

Propulsion–Airframe Integration

The low-speed turbine-based TRJ and dual-mode SJ are integrated in a dual (over/under) arrangement, which is a widely accepted method[18,19,30] for integrating multiple-engine flowpaths. This was chosen to demonstrate one possible configuration within the methodology, although several alternative combinations may eventually be possible for HICAD.

The inlet for the TRJ is integrated with the SJ with flow diverters such as moveable flaps to direct the air to the TRJ for $0 < M_0 \leq 5$ and to the SJ for $5 < M_0 < 10$ with a transition phase at Mach 5, where a parallel operation of the TRJ and SJ is anticipated. Rectangular inlet designs are generally easier for airframe integration. This engine arrangement is illustrated in the front and side views in Figs. 13 and 14, respectively. Actuators will be required to move the ramps during off-design operation.

The specific thrust graph of Fig. 15 provides the data to determine the mass flow ratio required to achieve the desired thrust at the SJ transition speed of Mach 5 at an altitude of 30 km. The plot is obtained using stream thrust analysis, which takes the fuel-to-air ratio as one its parameters. It relies on momentum relationships and

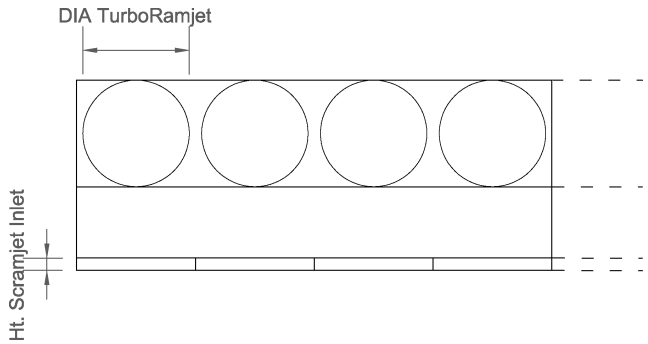

Fig. 13 TRJ–SJ integration (front view).

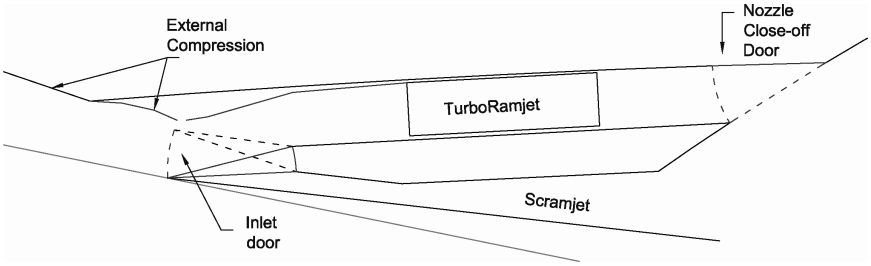

Fig. 14 TRJ–SJ integration (side view).

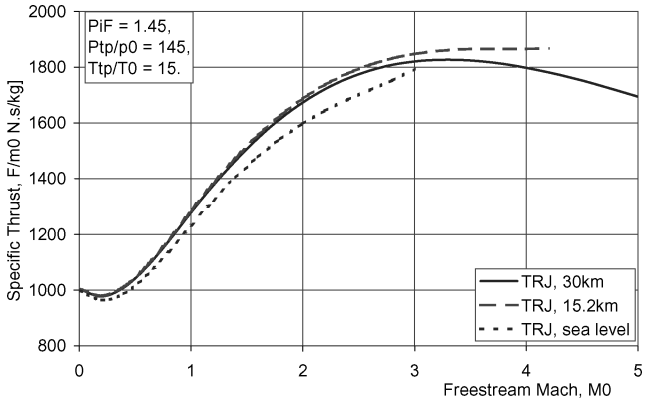

Fig. 15 Specific thrust at different altitudes.

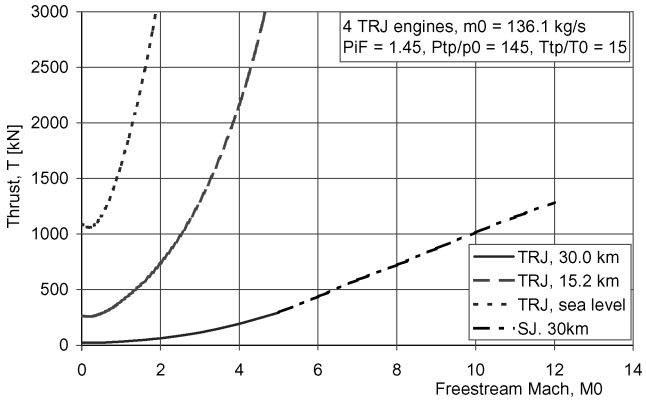

Fig. 16 Thrust matching of low-speed and high-speed engine.

a control volume that represents the on-design freestream capture area to nozzle exit area. It is assumed that the velocity vector is aligned with the local axial direction with the throughflow area perpendicular to that direction. The thrust produced by the SJ during constant-altitude acceleration is shown in Fig. 16. along with the thrust curves for the TRJ at different altitudes. Given that four TRJ units are used, each with a design $\dot{m}_0 = 136$ kg/s, that translates to a reference area of $A_{0_{\text{ref}}} = 0.98$ m^2.

The objective of the low-speed system is to provide adequate thrust for takeoff and transonic/supersonic acceleration to the high-speed propulsion system transition Mach number. The low-speed system will cease operation above transition and so mechanisms need to be employed to prevent airflow through the low-speed inlet system and divert it to the SJ during hypersonic flight. The nozzle is also highly integrated with the airframe and operates only during TRJ operation. Above transition, the nozzle closes and forms part of the high-speed nozzle system as shown in Fig. 14. The length and height of the nozzle, as shown in Fig. 7, are determined by subtracting the dimensions of the forebody and combustor length from the total vehicle length. The shape of the nozzle upper surface affects the magnitude of produced lift and the cowl needs to be positioned to maximize the lift.

Further Work

The development of HICAD will continue to achieve a holistic design methodology that maintains accuracy and improves its capabilities. This includes initial sizing, system packaging, weights and low-speed aerodynamics, stability, and performance while optimizing the resulting vehicles for the hypersonic cruise case. These improvements will not compromise HICAD's ease of use, flexibility, and ability to produce rapid results.

The current study focuses on the on-design cruise case only for the hypersonic regime, and further investigations will be carried out to look at improved variable-inlet geometry and total pressure recovery estimation for off-design performance. The vehicle is currently assumed to fly a constant dynamic pressure trajectory and that will be extended when the low-speed aerodynamic characteristics are fully explored. Other issues that will be incorporated into HICAD will include packaging of subsystems and trim analysis.

The methodology is limited to the conically derived waverider, which has a smaller vehicle volume compared to equivalent osculating-cone concepts, but it could be extended to also include these provided the run time required to produced optimized configurations does not prove too excessive. Other variables will be included to extend the optimization investigation such as the engine size and the axial location of the inlet plane.

It is envisaged that the optimization process will also be extended to consider alternative merit functions. The vehicle design is highly dependent on optimization to produce significantly better configurations to capture the synergies among various contributing design disciplines.

Conclusions

An airframe–propulsion integration methodology has been presented that integrates multiple engine flowpaths with a conically derived waverider airframe. This has been used to demonstrate a part of HICAD's overall design methodology for the preliminary design of operational hypersonic cruise aircraft concepts with horizontal takeoff and landing capabilities. A turbine-based TRJ has been used in conjunction with a dual-mode SJ to provide thrust for the full Mach range of flight from takeoff to Mach 9 or 10.

The SJ and TRJ are integrated with the lower part of the waverider airframe in an over/under configuration. This is one of a number of possibilities for integrating the two powerplants and HICAD will eventually offer the flexibility of using alternative arrangements.

This methodology offers user flexibility with emphasis placed on rapid results through employing well-established quasi-one-dimensional SJ combustor analysis and idealized cycle analysis for the TRJ. Oblique shock theory is used for the compression surfaces with planar shocks. The thrust of the two engines has been matched such that a smooth transition can occur between the low- and high-speed engine states at a predefined transition speed. The nonlinear simplex method has been used to geometrically optimize the generated hypersonic vehicle configuration and was successfully applied to a Mach 9 baseline waverider.

References

[1]Dornheim, M. A., "A Breath of Fast Air," *Aviation Week and Space Technology*, Vol. 160, No. 14, 2004, p. 28.

[2]Bertin, J. J., and Cummings, R. M., "Fifty Years of Hypersonics: Where We've Been, Where We're Going," *Progress in Aerospace Sciences*, Vol. 39, No. 6–7, 2003, pp. 511–536.

[3]Blankson, I., "Air-Breathing Hypersonic Cruise: Prospects for Mach 4-7 Waverider Aircraft," *Journal of Engineering for Gas Turbines and Power*, Vol. 116, No. 1, 1994, pp. 104–115.

[4]Bradford, J. E., and Olds, J. R., "SCCREAM v.5: A Web-Based Airbreathing Propulsion Analysis Tool," AIAA Paper 99-2104, June 1999.

[5]O'Brien, T. F., and Lewis, M. J., "Rocket-Based Combined-Cycle Engine Integration on an Osculating Cone Waverider Vehicle," *Journal of Aircraft*, Vol. 38, No. 6, 2001, pp. 1117–1123.

[6]Starkey, R. P., and Lewis, M. J., "Critical Design Issues for Airbreathing Hypersonic Waverider Missiles," *Journal of Spacecraft and Rockets*, Vol. 38, No. 4, 2001, pp. 510–519.

[7]Carreiro, L., "PDWAP—A Preliminary Design and Weights Analysis Program for Aerospace Vehicles," Technical Rept. AD-A222 614, Wright–Patterson AFB, OH, Jan. 1990.

[8]Molvik, G., Bowles, J., and Huynh, L., "Analysis of a Hypersonic Research Vehicle with a Hydrocarbon Scramjet Engine," AIAA Paper 93-0509, Jan. 1993.

[9]O'Neill, M. K. L., and Lewis, M., "Optimized Scramjet Integration on a Waverider," *Journal of Aircraft*, Vol. 9, No. 6, 1992, pp. 1114–1121.

[10]Takashima, N., and Lewis, M. J., "Optimization of Waverider-Based Hypersonic Cruise Vehicles with Off-Design Considerations," *Journal of Aircraft*, Vol. 36, No. 1, 1999, pp. 235–245.

[11]Horton, I., *Beginning Visual C++ 6*, Wiley, Indianapolis, IN, 1998, Chaps. 13–18.

[12]O'Neill, M. K. L., and Lewis, M., "Design Tradeoffs on Scramjet Engine Integrated Hypersonic Waverider Vehicles," *Journal of Aircraft*, Vol. 30, No. 6, 1993, pp. 943–952.

[13]Heiser, W. H., and Pratt, D. T., *Hypersonic Airbreathing Propulsion*, AIAA, Washington, DC, 1994, pp. 277–385.

[14]Mattingly, J. D., and Heiser, W. H., and Daley, D. H., *Aircraft Engine Design*, AIAA, New York, 1987, pp. 353–395.

[15]Bowcutt, K. G., "Hypersonic Aircraft Optimization Including Aerodynamic, Propulsion, and Trim Effects," AIAA Paper 92-5055, Dec. 1992.

[16]Bowcutt, K. G., "A Perspective on the Future of Aerospace Vehicle Design," AIAA Paper 2003-6957, Dec. 2003.

[17]Anderson, J. D., *Modern Compressible Flow: With Historical Perspective*, McGraw–Hill, Singapore, 1990, pp. 311–331.

[18]Moses, P. L., Bouchard, K. A., Vause, R. F., and Pinckney, S. Z., "An Airbreathing Launch Vehicle Design with Turbine-Based Low-Speed Propulsion and Dual Mode Scramjet High-Speed Propulsion," AIAA Paper 99-4948, Nov. 1999.

[19]Cockrell, C. R., Auslender, A. H., and McClinton, C. R., "Technology Roadmap for Dual-Mode Scramjet Propulsion to Support Space-Access Vision Vehicle Development," AIAA Paper 2002-5188, Sept. 2002.

[20]Billig, F. S., "Research on Supersonic Combustion," *Journal of Propulsion and Power*, Vol. 9, No. 4, 1993, pp. 499–514.

[21]O'Brien, T. F., and Lewis, M. J., "Quasi-One-Dimensional High-Speed Engine Model with Finite-Rate Chemistry," *Journal of Propulsion and Power*, Vol. 17, No. 6, 2001, pp. 1366–1374.

[22]Shapiro, A. H., *The Dynamics and Thermodynamics of Compressible Fluid Flow*, Vol. 1, Ronald, New York, 1953, pp. 219–231.

[23]Small, W. J., Weidner, J. P., and Johnston, P., "Scramjet Nozzle Design and Analysis as Applied to a Highly Integrated Hypersonic Research Airplane," NASA TN D-8334, No. 1976.

[24]Hunt, J., and McClinton, C., "Scramjet Engine/Airframe Integration Methodology, AGARD CP-479, April 1997.

[25]Tanatsugu, N., "Development Study on Air TurboRamjet," *Developments in High-Speed-Vehicle Propulsion Systems*, edited by S. Murthy and E. Curran, Vol. 165, Progress in Astronautics and Aeronautics, AIAA, Reston, VA, 1996, pp. 259–332.

[26]Hewitt, F., and Johnson, M., "Propulsion System Performance and Integration for High Mach Air Breathing Flight," *High-Speed Flight Propulsion Systems*, edited by S. Murthy and E. Curran, Vol. 137, Progress in Astronautics and Aeronautics, AIAA, Washington DC, 1991, pp. 101–142.

[27]Pegg, R. J., Hunt, J. L., and Petley, D. H., "Design of a Hypersonic Waverider-Derived Airplane," AIAA Paper 93-0401, Jan. 1993.

[28]Javaid, K. H., and Serghides, V. C., "Thrust-Matching Requirements for the Conceptual Design of Hypersonic Waverider Vehicles," AIAA Paper 2003-6953, Dec. 2003.

[29]Nelder, J., and Mead, R., "A Simplex Method for Function Minimization," *Computer Journal*, Vol. 7, Jan. 1965, pp. 308–313.

[30]Espinosa, A. M., "Hypersonic Airbreathing Propulsion: Mach 10 Cruiser Conceptual Design/Integration," AIAA Paper 93-4735, Aug. 1993.

J. Martin
Associate Editor